The Astrophysical Journal, 768:129 (7pp), 2013 May 10 doi:10.1088/0004-637X/768/2/129

MICROLENSING DISCOVERY OF A POPULATION OF VERY TIGHT, VERY LOW MASS BINARY BROWN DWARFS

J.-Y. Choi[1], C. Han[1,60,67], A. Udalski[2,61], T. Sumi[3,62], B. S. Gaudi[4,60], A. Gould[4,60], D. P. Bennett[5,62], M. Dominik[6,63,64,65], J.-P. Beaulieu[7,66], Y. Tsapras[8,9,64], V. Bozza[10,11,63], and F. Abe[12], I. A. Bond[13], C. S. Botzler[14], P. Chote[15], M. Freeman[14], A. Fukui[16], K. Furusawa[12], Y. Itow[12], C. H. Ling[13], K. Masuda[12], Y. Matsubara[12], N. Miyake[12], Y. Muraki[12], K. Ohnishi[17], N. J. Rattenbury[14], To. Saito[18], D. J. Sullivan[15], K. Suzuki[12], W. L. Sweatman[13], D. Suzuki[3], S. Takino[12], P. J. Tristram[19], K. Wada[3], P. C. M. Yock[14] (The MOA Collaboration), M. K. Szymański[2], M. Kubiak[2], G. Pietrzyński[2,20], I. Soszyński[2], J. Skowron[4], S. Kozłowski[2], R. Poleski[2], K. Ulaczyk[2], Ł. Wyrzykowski[2,21], P. Pietrukowicz[2] (The OGLE Collaboration), L. A. Almeida[22], D. L. DePoy[23], Subo Dong[24], E. Gorbikov[25], F. Jablonski[22], C. B. Henderson[4], K.-H. Hwang[1], J. Janczak[26], Y.-K. Jung[1], S. Kaspi[25], C.-U. Lee[27], U. Malamud[25], D. Maoz[25], D. McGregor[4], J. A. Muñoz[28], B.-G. Park[27], H. Park[1], R. W. Pogge[4], Y. Shvartzvald[25], I.-G. Shin[1], J. C. Yee[4] (The μFUN Collaboration), K. A. Alsubai[29], P. Browne[6], M. J. Burgdorf[30], S. Calchi Novati[31], P. Dodds[6], X.-S. Fang[32], F. Finet[33], M. Glitrup[34], F. Grundahl[34], S.-H. Gu[32], S. Hardis[35], K. Harpsøe[35,36], T. C. Hinse[27,35], A. Hornstrup[37], M. Hundertmark[6,38], J. Jessen-Hansen[34,39], U. G. Jrgensen[35,36], N. Kains[6,40], E. Kerins[41], C. Liebig[6,42], M. N. Lund[34], M. Lundkvist[34], G. Maier[42], L. Mancini[11,43], M. Mathiasen[35], M. T. Penny[4,41], S. Rahvar[44,45], D. Ricci[33,46], G. Scarpetta[10,31], J. Skottfelt[35], C. Snodgrass[47,48], J. Southworth[49], J. Surdej[33], J. Tregloan-Reed[49], J. Wambsganss[42], O. Wertz[33], F. Zimmer[42] (The MiNDSTEp Consortium), M. D. Albrow[50], E. Bachelet[51], V. Batista[4], S. Brillant[48], A. Cassan[52], A. A. Cole[53], C. Coutures[52], S. Dieters[53], D. Dominis Prester[54], J. Donatowicz[55], P. Fouqué[51], J. Greenhill[53], D. Kubas[48,52], J.-B. Marquette[52], J. W. Menzies[56], K. C. Sahu[57], M. Zub[42] (The PLANET Collaboration), D. M. Bramich[58], K. Horne[6], I. A. Steele[59], R. A. Street[8] (The RoboNet Collaboration),

[1] Department of Physics, Institute for Astrophysics, Chungbuk National University, Cheongju 371-763, Republic of Korea
[2] Warsaw University Observatory, Al. Ujazdowskie 4, 00-478 Warszawa, Poland
[3] Department of Earth and Space Science, Osaka University, Osaka 560-0043, Japan
[4] Department of Astronomy, Ohio State University, 140 West 18th Avenue, Columbus, OH 43210, USA
[5] Department of Physics, University of Notre Dame, 225 Nieuwland Science Hall, Notre Dame, IN 46556-5670, USA
[6] SUPA, School of Physics & Astronomy, University of St Andrews, North Haugh, St Andrews KY16 9SS, UK
[7] Institut dAstrophysique de Paris, UMR7095 CNRS–Université Pierre & Marie Curie, 98 bis boulevard Arago, F-75014 Paris, France
[8] Las Cumbres Observatory Global Telescope Network, 6740B Cortona Drive, Goleta, CA 93117, USA
[9] School of Physics and Astronomy, Queen Mary University of London, Mile End Road, London E1 4NS, UK
[10] INFN, Sezione di Napoli, I-80126 Napoli, Italy
[11] Dipartimento di Fisica E.R. Caianiello, Università di Salerno, Via Ponte Don Melillo, I-84084 Fisciano (SA), Italy
[12] Solar-Terrestrial Environment Laboratory, Nagoya University, Nagoya 464-8601, Japan
[13] Institute of Information and Mathematical Sciences, Massey University, Private Bag 102-904, North Shore Mail Centre, Auckland 0745, New Zealand
[14] Department of Physics, University of Auckland, Private Bag 92-019, Auckland 1001, New Zealand
[15] School of Chemical and Physical Sciences, Victoria University, Wellington 6140, New Zealand
[16] Okayama Astrophysical Observatory, National Astronomical Observatory of Japan, Asakuchi, Okayama 719-0232, Japan
[17] Nagano National College of Technology, Nagano 381-8550, Japan
[18] Tokyo Metropolitan College of Aeronautics, Tokyo 116-8523, Japan
[19] Mt. John University Observatory, P.O. Box 56, Lake Tekapo 8770, New Zealand
[20] Departamento de Astronomia, Universidad de Concepci'on, Casilla 160-C, Concepción, Chile
[21] Institute of Astronomy, University of Cambridge, Madingley Road, Cambridge CB3 0HA, UK
[22] Instituto Nacional de Pesquisas Espaciais, São José dos Campos, SP, Brazil
[23] Department of Physics, Texas A&M University, College Station, TX 77843, USA
[24] Institute for Advanced Study, Einstein Drive, Princeton, NJ 08540, USA
[25] School of Physics and Astronomy and Wise Observatory, Tel-Aviv University, Tel-Aviv 69978, Israel
[26] Department of Physics, Ohio State University, 191 W. Woodruff, Columbus, OH 43210, USA
[27] Korea Astronomy and Space Science Institute, Daejeon 305-348, Republic of Korea
[28] Departamento de Astronomìa y Astrofisica, Universidad de Valencia, E-46100 Burjassot, Valencia, Spain
[29] Qatar Foundation, P.O. Box 5825, Doha, Qatar
[30] HE Space Operations, Flughafenallee 24, D-28199 Bremen, Germany
[31] Istituto Internazionale per gli Alti Studi Scientifici (IIASS), I-84019 Vietri Sul Mare (SA), Italy
[32] National Astronomical Observatories/Yunnan Observatory, Key Laboratory for the Structure and Evolution of Celestial Objects, Chinese Academy of Sciences, Kunming 650011, China
[33] Institut dAstrophysique et de Géophysique, Allé du 6 Août 17, Sart Tilman, Bât. B5c, B-4000 Liége, Belgium
[34] Stellar Astrophysics Center (SAC), Department of Physics and Astronomy, Aarhus University, Ny Munkegade 120, DK-8000 Århus C, Denmark

[35] Niels Bohr Institute, University of Copenhagen, Juliane Maries vej 30, DK-2100 Copenhagen, Denmark
[36] Centre for Star and Planet Formation, Geological Museum, ster Voldgade 5, DK-1350 Copenhagen, Denmark
[37] Institut for Rumforskning og-teknologi, Danmarks Tekniske Universitet, Juliane Maries Vej 30, DK-2100 København, Denmark
[38] Institut für Astrophysik, Georg-August-Universität, Friedrich-Hund-Platz 1, D-37077 Göttingen, Germany
[39] Nordic Optical Telescope, Apartado 474, E-38700 Santa Cruz de La Palma, Spain
[40] ESO Headquarters, Karl-Schwarzschild-Str. 2, D-85748 Garching bei München, Germany
[41] Jodrell Bank Centre for Astrophysics, University of Manchester, Oxford Road, Manchester M13 9PL, UK
[42] Astronomisches Rechen-Institut, Zentrum für Astronomie der Universität Heidelberg (ZAH), Mönchhofstr. 12-14, D-69120 Heidelberg, Germany
[43] Max Planck Institute for Astronomy, Königstuhl 17, D-69117 Heidelberg, Germany
[44] Department of Physics, Sharif University of Technology, P.O. Box 11155–9161, Tehran, Iran
[45] Perimeter Institute for Theoretical Physics, 31 Caroline Street North, Waterloo, ON N2L2Y5, Canada
[46] INAF/Istituto di Astrofisica Spaziale e Fisica Cosmica–Bologna, Via Gobetti 101, I-40129 Bologna, Italy
[47] Max Planck Institute for Solar System Research, Max-Planck-Str. 2, D-37191 Katlenburg-Lindau, Germany
[48] European Southern Observatory (ESO), Alonso de Cordova 3107, Casilla 19001, Santiago 19, Chile
[49] Astrophysics Group, Keele University, Staffordshire ST5 5BG, UK
[50] Department of Physics and Astronomy, University of Canterbury, Private Bag 4800, Christchurch 8020, New Zealand
[51] IRAP, Université de Toulouse, CNRS, 14 Avenue Edouard Belin, F-31400 Toulouse, France
[52] UPMC-CNRS, UMR 7095, Institut dAstrophysique de Paris, 98bis boulevard Arago, F-75014 Paris, France
[53] School of Mathematics and Physics, University of Tasmania, Private Bag 37, Hobart, TAS 7001, Australia
[54] Department of Physics, University of Rijeka, Omladinska 14, 51000 Rijeka, Croatia
[55] Department of Computing, Technical University of Vienna, Wiedner Hauptstrasse, A-1040 Vienna, Austria
[56] South African Astronomical Observatory, P.O. Box 9, Observatory 7925, South Africa
[57] Space Telescope Science Institute, 3700 San Martin Drive, Baltimore, MD 21218, USA
[58] European Southern Observatory, Karl-Schwarzschild-Str. 2, D-85748 Garching bei München, Germany
[59] Astrophysics Research Institute, Liverpool John Moores University, Liverpool CH41 1LD, UK
Received 2013 February 18; accepted 2013 March 22; published 2013 April 23

ABSTRACT

Although many models have been proposed, the physical mechanisms responsible for the formation of low-mass brown dwarfs (BDs) are poorly understood. The multiplicity properties and minimum mass of the BD mass function provide critical empirical diagnostics of these mechanisms. We present the discovery via gravitational microlensing of two very low mass, very tight binary systems. These binaries have directly and precisely measured total system masses of 0.025 $M_{\odot}$ and 0.034 $M_{\odot}$, and projected separations of 0.31 AU and 0.19 AU, making them the lowest-mass and tightest field BD binaries known. The discovery of a population of such binaries indicates that BD binaries can robustly form at least down to masses of $\sim$0.02 $M_{\odot}$. Future microlensing surveys will measure a mass-selected sample of BD binary systems, which can then be directly compared to similar samples of stellar binaries.

Key words: binaries: general – gravitational lensing: micro

Online-only material: color figures

1. INTRODUCTION

Brown dwarfs (BDs) are collapsed objects with masses below the minimum mass required to fuse hydrogen of $\sim$0.08 $M_{\odot}$. Direct imaging surveys have found that isolated BD systems to be fairly ubiquitous in the field as well as in young clusters (see Luhman 2012 for a review), with frequencies rivaling those of their more massive hydrogen-fusing stellar brethren. However, it is unclear whether BDs simply represent the low-mass extension of the initial collapsed object mass function (IMF), and thus formed via the same processes as stars, or if their formation requires additional physical mechanisms.

The minimum mass of the IMF potentially provides an important discriminant between various models of BD formation, with very low mass BD binary systems being particularly important in this regard. This is because predictions for the multiplicity properties of low-mass BDs—frequency, mass ratio, and separation as a function of total system mass and age—differ significantly depending on the formation scenario. However, the currently available observational samples are strongly influenced by detection biases and selection effects. For example, although BD surveys in young stellar associations allow for detections of low-mass BD systems, these associations are typically fairly distant, making it difficult to detect tight BD binaries. Conversely, field BD binaries can be resolved to much smaller separations, but low-mass, old field BDs are quite faint and thus difficult to detect. As a result, the current sample of binary BDs is not only small in number but also substantially incomplete, particularly in the regime of low mass and small separation. A further complication is that direct mass measurements are available only for a subset of tight field BD binaries. Mass estimates of other systems must rely on comparison with models, resulting in substantial systematic uncertainties.

Gravitational microlensing is well suited to fill the gap. Microlensing is the astronomical phenomenon wherein the brightness of a star is magnified by the bending of light caused by the gravity of an intervening object (lens) located between the background star (source) and an observer. Since this effect occurs regardless of the lens brightness, microlensing is suitable for detecting faint objects such as BDs (Paczyński 1986). For a lensing event produced by a binary lens with well-resolved brightness variation of the lensed star, it is possible to

[60] The μFUN Collaboration.
[61] The OGLE Collaboration.
[62] The MOA Collaboration.
[63] The MiNDSTEp Consortium.
[64] The RoboNet Collaboration.
[65] Royal Society University Research Fellow.
[66] The PLANET Collaboration.
[67] Corresponding author.

Table 1
Telescopes

Event	Telescope
OGLE-2009-BLG-151	MOA, 1.8 m Mt. John, New Zealand
/MOA-2009-BLG-232	OGLE, 1.3 m Warsaw, Las Campanas, Chile
	μFUN, 1.3 m SMARTS, Cerro Tololo Inter-American (CTIO), Chile
	μFUN, 1.0 m Mt. Lemmon, USA
	PLANET, 1.0 m Canopus, Australia
	PLANET, 1.0 m South African Astronomical (SAAO), South Africa
	PLANET, 0.6 m Perth, Australia
	MiNDSTEp, 1.54 m Danish, La Silla, Chile
	RoboNet, 2.0 m Faulkes North Telescope (FTN), Hawaii, USA
	RoboNet, 2.0 m Faulkes South Telescope (FTS), Hawaii, USA
	RoboNet, 2.0 m Liverpool Telescope (LT), Canary Islands, Spain
OGLE-2011-BLG-0420	OGLE, 1.3 m Warsaw, Las Campanas, Chile
	MOA, 0.6 m B&C, Mt. John, New Zealand
	μFUN, 1.3 m SMARTS, CTIO, Chile
	μFUN, 1.0 m Wise, Israel
	PLANET, 1.0 m SAAO, South Africa
	PLANET, 1.0 m Canopus, Australia
	MiNDSTEp, 1.54 m Danish, La Silla, Chile
	RoboNet, 2.0 m LT, Canary Islands, Spain

precisely measure the physical parameters of the lensing object including the mass and distance. Here we report the discovery and characterization of two binary BD systems, both of which have very low mass and tight separation, thus constituting a new population.

2. OBSERVATION

These BD binaries were discovered in microlensing events OGLE-2009-BLG-151/MOA-2009-BLG-232 and OGLE-2011-BLG-0420. The events occurred on stars located in the Galactic bulge field with equatorial and Galactic coordinates (R.A., decl.)$_{2000}$ = ($17^{\rm h}54^{\rm m}22\overset{\rm s}{.}34$, $-29°03'20\overset{''}{.}8$), $(l, b)_{2000}$ = ($0\overset{\circ}{.}88, -1\overset{\circ}{.}70$) and (R.A., decl.)$_{2000}$ = ($17^{\rm h}50^{\rm m}56\overset{\rm s}{.}18$, $-29°49'30\overset{''}{.}2$), $(l, b)_{2000}$ = ($359\overset{\circ}{.}84, -1\overset{\circ}{.}45$), respectively.

OGLE-2009-BLG-151/MOA-2009-BLG-232 was first discovered by the Optical Gravitational Lensing Experiment (OGLE; Udalski 2003) group and was independently discovered by the Microlensing Observations in Astrophysics (MOA; Bond et al. 2001; Sumi et al. 2003) group in 2009 observation season. OGLE-2011-BLG-0420 was detected by the OGLE group in the 2011 season. Both events were additionally observed by follow-up observation groups including Microlensing Follow-Up Network (μFUN; Gould et al. 2006), Probing Lensing Anomalies NETwork (PLANET; Beaulieu et al. 2006), RoboNet (Tsapras et al. 2009), and Microlensing Network for the Detection of Small Terrestrial Exoplanets (MiNDSTEp; Dominik et al. 2010). In Table 1, we list the survey and follow-up groups along with their telescope characteristics. Data reductions were carried out using photometry codes developed by the individual groups.

3. ANALYSIS

Figure 1 displays the light curves of the individual events. OGLE-2009-BLG-151/MOA-2009-BLG-232 is characterized by two strong spikes flanking a "U"-shaped trough, which is typical for caustic-crossing binary-lens events. Caustics denote positions on the source plane where the lensing magnification of a point source diverges (Petters et al. 2001). When a caustic is formed by an astronomical object composed of two masses,

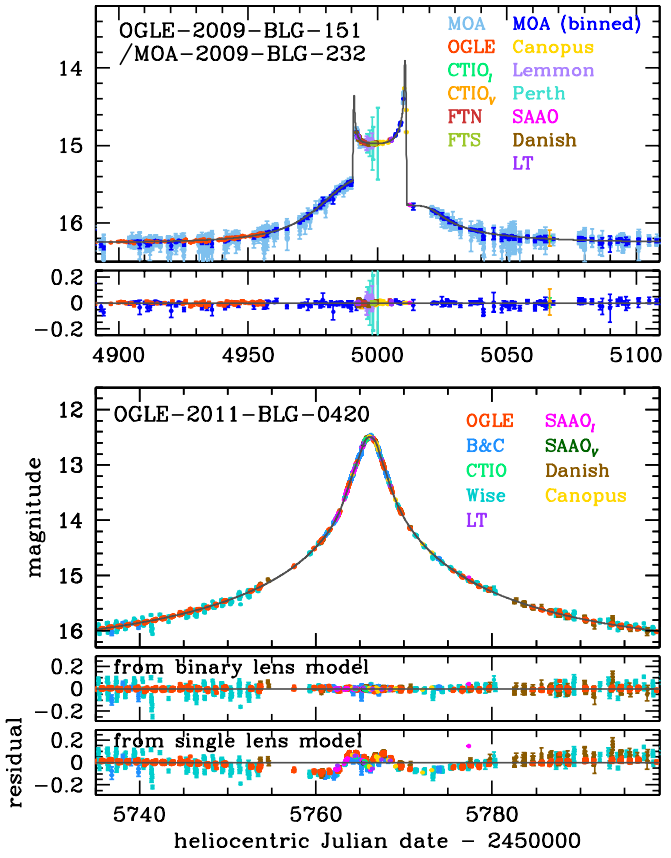

Figure 1. Light curves of the binary BD microlensing events OGLE-2009-BLG-151/MOA-2009-BLG-232 and OGLE-2011-BLG-0420. For the MOA data of OGLE-2009-BLG-151/MOA-2009-BLG-232, binned data are additionally plotted to better show residuals.

(A color version of this figure is available in the online journal.)

it forms a single set or multiple sets of closed curves each consisting of concave curves that meet at cusps. When a source star crosses the caustic, its brightness is greatly enhanced, causing strong deviation from the smooth and symmetric single-lens light curve. The light curve of OGLE-2011-BLG-0420, on

the other hand, appears to be smooth and symmetric, which are the characteristics of a lensing event caused by a single mass. From the fit based on the single-lens model, however, the light curve exhibits noticeable deviations near the peak, which indicates the existence of a companion to the lens. According to the classification scheme of binary signatures in lensing light curves set by Ingrosso et al. (2009), the deviations of OGLE-2009-BLG-151/MOA-2009-BLG-232 and OGLE-2011-BLG-0420 are classified as Classes II and I, respectively.

With known binary signatures, we conduct binary-lens modeling of the observed light curves. For a single lens, the light curve is described by three parameters: the time of closest lens–source approach, t_0; the lens–source separation (normalized by the Einstein-ring radius, $\theta_{\rm E}$) at that time, u_0; and the Einstein timescale, $t_{\rm E}$, which represents the time required for the source to cross $\theta_{\rm E}$. The Einstein ring denotes the image of a source in the event of perfect lens–source alignment, and so is used as the length scale of lensing phenomena. Binary lenses require three additional parameters: the mass ratio, q; the projected separation (normalized by $\theta_{\rm E}$) between the binary components, s; and the angle between the source trajectory and the binary axis, α (source trajectory angle).

In addition to the basic lensing parameters, it is often necessary to include additional parameters to precisely describe subtle light curve features caused by various second-order effects. For both events, the lensing-induced magnification lasted for several months, which comprises a significant fraction of Earth's orbital period around the Sun (1 year). Then, the apparent motion of the source with respect to the lens deviates from rectilinear (Gould 1992) due to the change of the observer's position caused by Earth's orbital motion. This parallax effect causes long-term deviation in the lensing light curves. Consideration of the parallax effect requires two additional parameters, $\pi_{{\rm E},N}$ and $\pi_{{\rm E},E}$, which are the two components of the lens parallax vector $\boldsymbol{\pi}_{\rm E}$, projected on the sky along the north and east equatorial coordinates, respectively. The orbital motion of the lens also affects lensing light curves. The lens orbital motion causes the projected binary separation and the source trajectory angle to change over the course of a lensing event. These require two additional lensing parameters of the change rates of the binary separation, ds/dt, and the source trajectory angle, $d\alpha/dt$. Finally, finite-source effects become important whenever the magnification varies very rapidly with the change of the source position, so that different parts of the source are magnified by different amounts. Such a rapid magnification variation occurs near caustics and thus finite-source effects are important for binary-lens events involved with caustic crossings or approaches. This requires one more parameter, the normalized source radius $\rho_* = \theta_*/\theta_{\rm E}$, where θ_* is the angular source radius. Measuring the deviation caused by the parallax and finite-source effects is important to determine the physical parameters of the lens. By measuring the finite-source effect, the Einstein radius is determined by $\theta_{\rm E} = \theta_*/\rho_*$ once the source radius is known. With the measured lens parallax and the Einstein radius, the mass and distance to the lens are determined as $M_{\rm tot} = \theta_{\rm E}/(\kappa\pi_{\rm E})$ and $D_{\rm L} = {\rm AU}/(\pi_{\rm E}\theta_{\rm E} + \pi_{\rm S})$, respectively (Gould 1992; Gould et al. 2006). Here $\kappa = 4G/(c^2{\rm AU})$, AU is an astronomical unit, $\pi_{\rm S} = {\rm AU}/D_{\rm S}$, and $D_{\rm S} \sim 8$ kpc is the source distance.

We model the observed light curves by minimizing χ^2 in the parameter space. We investigate the existence of possible degenerate solutions because it is known that light curves resulting from different combinations of lensing parameters often result in similar shapes (Griest & Safazadeh 1998; Dominik 1999; An 2005). In modeling finite-source effects, we additionally consider the limb-darkening variation of the source star surface (Witt 1995) by modeling the surface profile as a standard linear law. For χ^2 minimization, we use the Markov Chain Monte Carlo method. Photometric errors of the individual data sets are rescaled so that the χ^2 per degree of freedom becomes unity for each data set. We eliminate data points with large errors and those lying beyond 3σ from the best-fit model to minimize their effect on modeling.

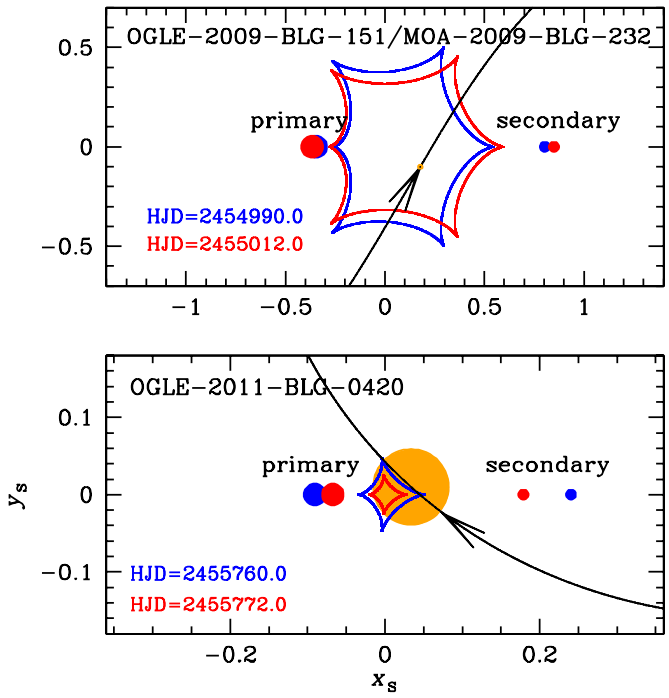

Figure 2. Geometry of the lens systems. In each panel, the cuspy closed figure represents the caustic, the small filled dots are the locations of the binary lens components, and the curve with an arrow represents the source trajectory. Two sets of lens positions and the corresponding caustics are presented at the times marked in the panel. The circle on the source trajectory represents the scale of the source star with respect to the caustic. All lengths are normalized by the Einstein radius corresponding to the total mass of the lens.

(A color version of this figure is available in the online journal.)

Table 2 gives the solutions of the lensing parameters found from modeling. In Figure 2, we also present the geometry of the lens system where the source trajectory with respect to the positions of the binary lens components and the caustic are shown. For OGLE-2009-BLG-151/MOA-2009-BLG-232, we find that the two strong spikes were produced by the source crossings of a big caustic formed by a binary lens with the projected separation between the lens components ($s \sim 1.14$) being similar to the Einstein radius of the lens. We find that including the second-order effects of lens parallax and orbital motions improves the fit by $\Delta\chi^2 = 213$. OGLE-2011-BLG-0420 is also a caustic-crossing event, but the projected binary separation ($s \sim 0.29$) is substantially smaller than the Einstein radius. For such a close binary lens, the caustic is small. For OGLE-2011-BLG-0420, the caustic is so small that the source size is similar to that of the caustic. Hence, the lensing magnification is greatly attenuated by the severe finite-source effect, and thus the deviation during the caustic crossings is weak. We find that there exists an alternative solution with $s > 1$ caused by the well-known close/wide binary degeneracy, but the degeneracy is resolved with $\Delta\chi^2 = 27$.

Table 2
Best-fit Lensing Parameters

Parameters	OGLE-2009-BLG-151 /MOA-2009-BLG-232	OGLE-2011-BLG-0420
χ^2/dof	3040.9/3032	5410.3/5439
t_0 (HJD′)	4999.680 ± 0.061	5766.110 ± 0.001
u_0	-0.217 ± 0.004	-0.030 ± 0.001
$t_{\rm E}$ (days)	27.95 ± 0.11	35.22 ± 0.08
s	1.135 ± 0.004	0.289 ± 0.002
q	0.419 ± 0.006	0.377 ± 0.009
α	-1.049 ± 0.004	-2.383 ± 0.002
ρ_* (10^{-2})	1.06 ± 0.01	4.88 ± 0.01
$\pi_{{\rm E},N}$	-3.33 ± 0.11	-1.15 ± 0.05
$\pi_{{\rm E},E}$	-0.91 ± 0.11	0.19 ± 0.01
ds/dt (yr^{-1})	1.55 ± 0.13	-2.59 ± 0.07
$d\alpha/dt$ (yr^{-1})	0.69 ± 0.06	6.88 ± 0.20
slope (mag yr^{-1})	0.0052 ± 0.0008	...

Note. HJD′ = HJD − 2,450,000.

Table 3
Source Star Properties

Quantity	OGLE-2009-BLG-151 /MOA-2009-BLG-232	OGLE-2011-BLG-0420
$(V-I)_0$	1.352	1.611
I_0	14.490	13.091
θ_* (μas)	7.57 ± 0.66	15.94 ± 1.38
Stellar type	K giant	K giant
$\theta_{\rm E}$ (mas)	0.71 ± 0.01	0.33 ± 0.03

The parallax and lens orbital effects are also clearly measured with $\Delta\chi^2 = 403$. From 10 years of OGLE data, we find that OGLE-2011-BLG-0420S (source star) is extremely stable, but OGLE-2009-BLG-151/MOA-2009-BLG-232S exhibits irregular <1% variations, typically on timescales of a few hundred days. Because these can affect the parallax measurement, we restrict the modeling to $t_0 \pm 300$ days to minimize the impact of variations while still retaining enough baseline to ensure a stable fit. We also include a "slope" parameter for the source flux to account for the remaining variability. We find only slight differences in final results if we repeat this procedure with longer baselines. Therefore, it is unlikely but not impossible that source variability affects the OGLE-2009-BLG-151/MOA-2009-BLG-232 parallax measurement. By contrast, the results for OGLE-2011-BLG-0420 are very robust.

4. PHYSICAL PARAMETERS

Since ρ_* and $\pi_{\rm E}$ are well measured (Table 2), it is possible to determine $M_{\rm tot}$ and $D_{\rm L}$ for both systems. The only missing ingredient is the angular source radius θ_*, which is needed to find $\theta_{\rm E} = \theta_*/\rho_*$. This is determined from the de-reddened color and brightness of the source star. For the calibration of the color and brightness, we use the centroid of bulge giant clump as a reference (Yoo et al. 2004) because its de-reddened brightness $I_{0,{\rm c}} = 14.45$ at the Galactocentric distance (Nataf et al. 2012) and the color $(V-I)_{0,{\rm c}} = 1.06$ (Bensby et al. 2011) are known. We then translate $V-I$ into $V-K$ color by using the relation. Once the $V-K$ color is known, the angular source radius θ_* is obtained the relation between the $V-K$ color and the angular radius provided by Kervella et al. (2004). In Table 3, we list the measured de-reddened colors $(V-I)_0$, magnitudes I_0, angular radii, types of the source stars, and the measured Einstein radii of the individual events. Figure 3 shows the locations of the lensed stars of the individual events on the color–magnitude diagrams.

Table 4
Physical Quantities

Quantity	OGLE-2009-BLG-151 /MOA-2009-BLG-232	OGLE-2011-BLG-0420
$M_{\rm tot}$ ($M_\odot$)	0.025 ± 0.001	0.034 ± 0.002
M_1 ($M_\odot$)	0.018 ± 0.001	0.025 ± 0.001
M_2 ($M_\odot$)	0.0075 ± 0.0003	0.0094 ± 0.0005
$D_{\rm L}$ (kpc)	0.39 ± 0.01	1.99 ± 0.08
$d_\perp$ (AU)	0.31 ± 0.01	0.19 ± 0.01

The derived physical quantities for the OGLE-2009-BLG-151/MOA-2009-BLG-232L and OGLE-2011-BLG-0420L binaries are listed in Table 4. Here the letter "L" at the end of each event indicates the lens of the event. The total system masses are $M_{\rm tot} = (0.025 \pm 0.001)\,M_\odot$ and $(0.034 \pm 0.002)\,M_\odot$, respectively, well below the hydrogen-burning limit. The projected separations and mass ratios are $d_\perp = (0.31 \pm 0.01)$ AU and $q = 0.419 \pm 0.006$ for OGLE-2009-BLG-151/MOA-2009-BLG-232L, and $d_\perp = (0.19 \pm 0.01)$ AU and $q = 0.377 \pm 0.009$ for OGLE-2011-BLG-0420L. It is worth emphasizing the high precisions (<10%) with which the total system masses and individual component masses are determined.

Figure 4 compares OGLE-2009-BLG-151/MOA-2009-BLG-232L and OGLE-2011-BLG-0420L to a sample of low-mass binaries in the field and in young associations from Faherty et al. (2011), Basri & Martín (1999), Burgasser et al. (2008, 2012), and Lane et al. (2001). The only known BD binaries with comparable total masses are Oph 16225-240515 with $M_{\rm tot} \sim 0.032\,M_\odot$ (Jayawardhana & Ivanov 2006) and 2MASSJ1207334-393254 (Chauvin et al. 2004) with $M_{\rm tot} \sim 0.028\,M_\odot$. However, these two systems are both young (5 Myr and 8 Myr, respectively) and have very wide separations of hundreds of AU. Indeed, OGLE-2009-BLG-151/MOA-2009-BLG-232L and OGLE-2011-BLG-0420L are the tightest known BD binaries with substantially lower mass than previously known field BD binaries. Both systems have mass ratios of ~0.4, apparently consistent with the trend found from old field BDs, which tend to have a preference for larger mass ratios (see Figure 3 of Burgasser et al. (2007)), although it is important to stress that the selection effects in microlensing and direct imaging surveys are very different.

Burgasser et al. (2007) suggested that field low-mass binaries with $M_{\rm tot} = 0.05$–$0.2\,M_\odot$ may exhibit an empirical lower limit to their binding energies of $Gm_1m_2/a \sim 2.5 \times 10^{42}$ erg (see Figure 5). Although OGLE-2009-BLG-151/MOA-2009-BLG-232L and OGLE-2011-BLG-0420L are substantially lower in mass than these BD binaries, they are also considerably tighter. Therefore, with binding energies of $\sim 7 \times 10^{42}$ erg and 2×10^{43} erg, they are consistent with the extrapolation of the minimum binding energy limit down to total system masses of $M_{\rm tot} \sim 0.02\,M_\odot$.

Although we are unable to provide an estimate of the space density of such tight, low-mass BD binaries, or even an estimate of their frequency relative to more massive stellar binaries, the discovery of two systems among the relatively small sample of binary lensing events with precise mass estimates strongly suggests that very low mass, very tight BD binaries are not rare. Thus, these detections herald a much larger population of such systems. We can therefore conclude that BD binaries can

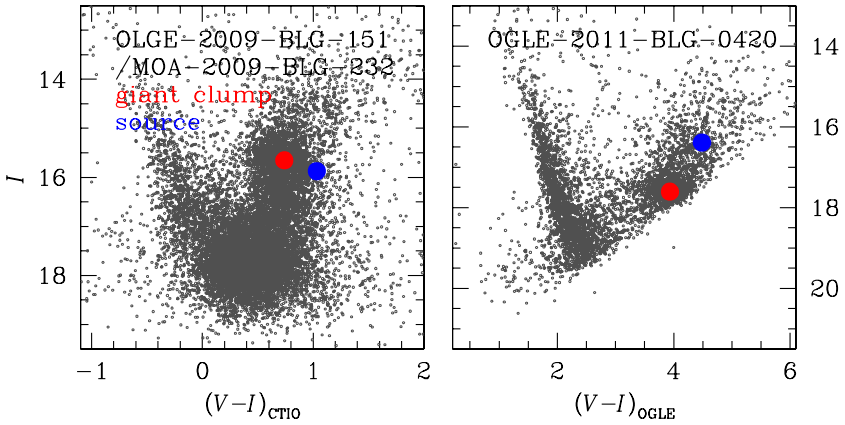

Figure 3. Locations of the lensed stars of the individual events on the color–magnitude diagrams.
(A color version of this figure is available in the online journal.)

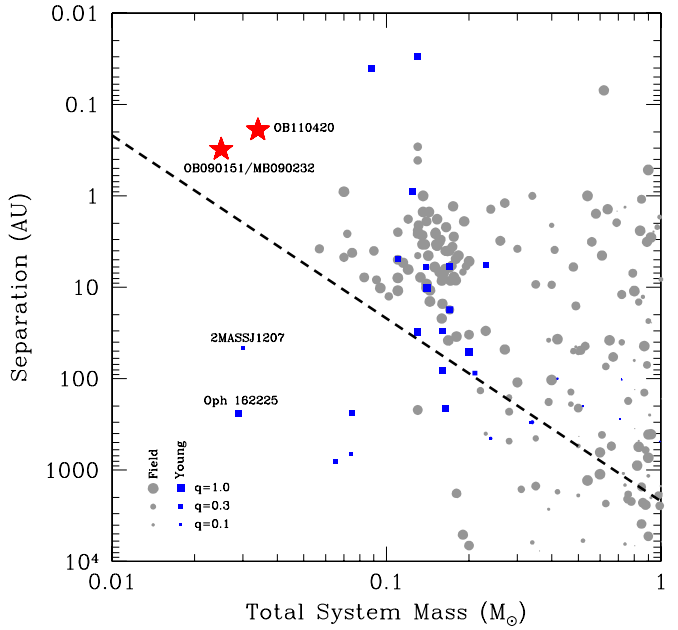

Figure 4. Projected separation vs. total system mass for a compilation of binaries. Gray circles indicate old field binaries, whereas blue squares indicate young (<500 Myr) systems. The size of the symbols is proportional to the square root of the mass ratio. The red stars are the two tight, low-mass binary BDs discussed here, which have mass ratios of ∼0.4. The dashed line shows a binding energy of 2×10^{42} erg, assuming a mass ratio of 1.
(A color version of this figure is available in the online journal.)

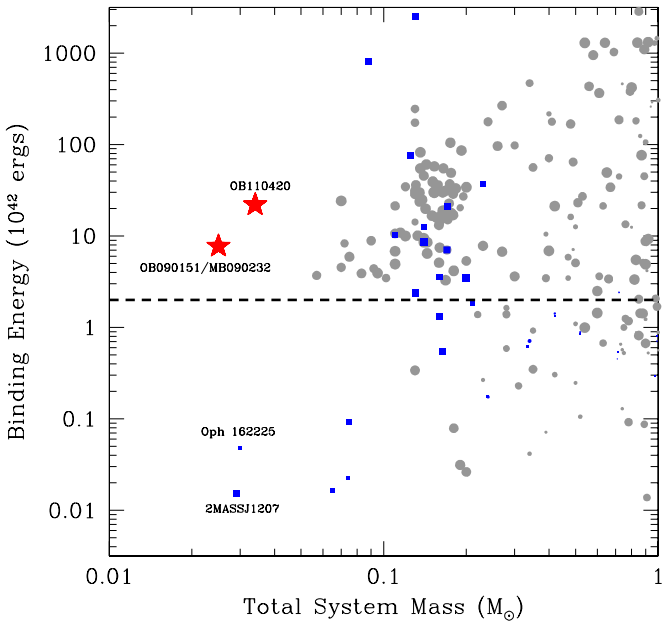

Figure 5. Binding energy (Gm_1m_2/a) vs. total system mass for the same binaries as shown in Figure 4. Symbols and line are the same.
(A color version of this figure is available in the online journal.)

robustly form at least down to system masses of $\sim 0.02\,M_\odot$, providing a strong constraint for formation models.

5. DISCUSSION

The discoveries of the binary BDs reported in this paper demonstrate the importance of microlensing in BD studies. The microlensing method has various advantages. First, it enables us to detect faint old populations of BDs that could not be studied by the conventional method of imaging surveys and the sensitivity extends down to planetary mass objects (Sumi et al. 2011). It also allows one to detect BDs distributed throughout the Galaxy. Therefore, microlensing enables us to study BDs based on a sample that is not biased by the brightness and distance. Second, in many cases of microlensing BDs, it is possible to precisely measure the mass, which is not only the most fundamental physical parameter but also a quantity enabling to unambiguously distinguish BDs from other low-mass populations such as low-mass stars. While mass measurements by the conventional method require long-term and multiple stage observation of imaging, astrometry, and spectroscopy by using space-borne or very large ground-based telescopes, microlensing requires simple photometry by using 1 m class telescopes. Despite the observational simplicity, the mass can be measured with uncertainties equivalent to or smaller than those of the measurement by conventional methods. Finally, microlensing can expand the ranges of masses and separations in the binary BD sample that is incomplete below $\sim 0.1\,M_\odot$ in mass and ∼3 AU in separation. Microlensing sensitivity to binary objects peaks when the separation is of the order of the Einstein radius. Considering that the Einstein radius corresponding to a typical binary BD is <1 AU, microlensing method will make it possible to study binary BDs with small separations.

The number of microlensing BDs is expected to increase in the future with the upgrade of instruments in the existing

survey experiments and the advent of new surveys. The OGLE group recently upgraded its camera with a wider field of view to significantly increase the observational cadence. The Korea Microlensing Telescope Network (KMTNet), now being constructed, will achieve 10 minute sampling of all lensing events by using a network of 1.6 m telescopes on three different continents in the Southern hemisphere with wide-field cameras. Furthermore, there are planned lensing surveys in space including *EUCLID* and *WFIRST*. With the increase of the microlensing event rate combined with the improved precision of observation, microlensing will become a major method to study BDs.

Work by C. Han was supported by the research grant of Chungbuk National University in 2011. The OGLE project has received funding from the European Research Council under the European Community's Seventh Framework Programme (FP7/2007-2013)/ERC grant agreement No. 246678. The MOA experiment was supported by grants JSPS22403003 and JSPS23340064. This work is based in part on data collected by MiNDSTEp with the Danish 1.54 m telescope at the ESO La Silla Observatory, which is operated based on a grant from the Danish Natural Science Foundation (FNU). The MiNDSTEp monitoring campaign is powered by ARTEMiS (Dominik et al. 2008). M.H. acknowledges support by the German Research Foundation (DFG). D.R. (boursier FRIA), F.F. (boursier ARC), and J. Surdej acknowledge support from the Communauté française de Belgique—Actions de recherche concertées—Académie universitaire Wallonie-Europe. K.A., D.M.B., M.D., K.H., M.H., C.L., C.S., R.A.S., and Y.T. are thankful to the Qatar National Research Fund (QNRF), member of the Qatar Foundation, for support by grant NPRP 09-476-1-078. C.S. has received funding from FP7/2007-2013 under grant agreement No. 268421. K.H. is supported by a Royal Society Leverhulme Trust Senior Research Fellowship. A.G. and B.S.G. acknowledge support from NSF AST-1103471. B.S.G., A.G., and R.W.P. acknowledge support from NASA grant NNX12AB99G. Work by J.C.Y. is supported by a National Science Foundation Graduate Research Fellowship under grant No. 2009068160. S.D.'s research was performed under contract with the California Institute of Technology funded by NASA through the Sagan Fellowship Program. T.S. was supported by the grant JSPS23340044. Y.M. acknowledges support from JSPS grants JSPS23540339 and JSPS19340058. T.C.H. and C.U.L. acknowledge the support of KASI grant 2012-1-410-02 and KRCF.

REFERENCES

An, J. H. 2005, MNRAS, 356, 1409
Basri, G., & Martín, E. L. 1999, AJ, 118, 2460
Beaulieu, J.-P., Bennett, D. P., Fouqué, P., et al. 2006, Natur, 439, 437
Bensby, T., Adén, D., Meléndez, J., et al. 2011, A&A, 533, 134
Bessell, M. S., & Brett, J. M. 1988, PASP, 100, 1134
Bond, I. A., Abe, F., Dodd, R. J., et al. 2001, MNRAS, 327, 868
Burgasser, A. J., Liu, M. C., Ireland, M. J., Cruz, K. L., & Dupuy, T. J. 2008, ApJ, 681, 579
Burgasser, A. J., Luk, C., Dhital, S., et al. 2012, ApJ, 757, 110
Burgasser, A. J., Reid, I. N., Siegler, N., et al. 2007, in Protostars and Planets, ed. V. J. Reipurth, D. Jewitt, & K. Keil (Tucson, AZ: Univ. Arizona Press), 427
Chauvin, G., Lagrange, A.-M., Dumas, C., et al. 2004, A&A, 425, L29
Dominik, M. 1999, A&A, 349, 108
Dominik, M., Horne, K., Allan, A., et al. 2008, AN, 329, 248
Dominik, M., Jørgensen, U. G., Rattenbury, N. J., et al. 2010, AN, 331, 671
Faherty, J. K., Burgasser, A. J., Bochanski, J. J., et al. 2011, AJ, 141, 71
Gould, A. 1992, ApJ, 392, 442
Gould, A., Udalski, A., An, D., et al. 2006, ApJ, 644, L37
Griest, K., & Safazadeh, N. 1998, ApJ, 500, 37
Ingrosso, G., Novati, S. C., de Paolis, F., et al. 2009, MNRAS, 399, 219
Jayawardhana, R., & Ivanov, V. D. 2006, Sci, 313, 1279
Kervella, P., Thévenin, F., Di Folco, E., & Ségransan, D. 2004, A&A, 426, 297
Lane, B. F., Zapatero Osorio, M. R., Britton, M. C., Martín, E. L., & Kulkarni, S. R. 2001, ApJ, 560, 390
Luhman, K. L. 2012, ARA&A, 50, 65
Nataf, D. M., Gould, A., Fouqué, P., et al. 2012, arXiv1208.1263
Paczyński, B. 1986, ApJ, 304, 1
Petters, A. O., Levine, H., & Wambsganss, J. 2001, Singularity Theory and Gravitational Lensing, Progress in Mathematical Physics, Vol. 21 (Boston, MA: Birkhäuser)
Sumi, T., Abe, F., Bond, I. A., et al. 2003, ApJ, 591, 204
Sumi, T., Kamiya, K., Bennett, D. P., et al. 2011, Natur, 473, 349
Tsapras, Y., Street, R., Horne, K., et al. 2009, AN, 330, 4
Udalski, A. 2003, AcA, 53, 291
Witt, H. J. 1995, ApJ, 449, 42
Yoo, J., DePoy, D. L., Gal-Yam, A., et al. 2004, ApJ, 603, 139